

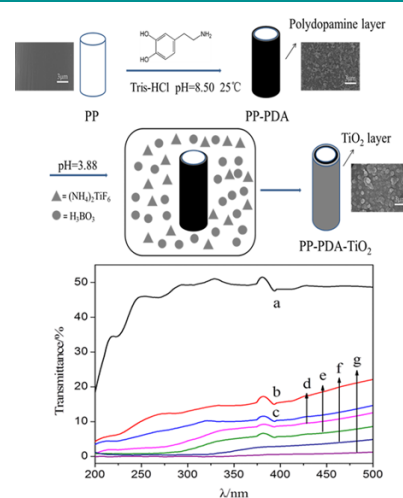
Mussel-Inspired Multifunctional Coating for Enhancing the UV-Resistant Property of Polypropylene Fibers

Zhengyi Liu
Juncheng Hu
Qi Sun
Li Chen
Xia Feng*
Yiping Zhao*

State Key Laboratory of Separation Membranes and Membrane Processes, School of Materials Science and Engineering, Tianjin Polytechnic University, Tianjin 300387, P. R. China

Received October 23, 2016 / Revised January 12, 2017 / Accepted February 6, 2017

Abstract: In this paper, UV-resistant polypropylene (PP) fibers were prepared with a simple and versatile strategy. The PP fiber was firstly coated a polydopamine (PDA) layer by simply dipping the fiber into an alkaline dopamine solution. Then, the titania (TiO_2) nanoparticles were chemically bound to the PDA layer through the reduction capacity of catechol groups in PDA, endowing the fibers with excellent UV-resistant properties. The surface chemical composition of modified fibers was confirmed by attenuated total reflectance fourier transform infrared (ATR-FTIR) spectroscopy and X-ray photoelectron spectroscopy (XPS). The surface morphology and the crystalline structure of the modified fibers were studied by scanning electron microscopy (SEM) and X-ray diffraction (XRD) respectively. Thermo stability was characterized by thermogravimetry analysis. Besides, the mechanical and UV protection properties were further investigated through monofilament tensile and the UV transmittance test. The results showed that the PDA and TiO_2 were successfully coated on fiber surface. Compared to the pristine fiber, the modified fiber exhibited better thermal stability. Particularly, the as-prepared PP-PDA- TiO_2 fibers could strongly resist the UV rays with no change in mechanical properties.



Keywords: polydopamine, titania, polypropylene fiber, UV protection property.

1. Introduction

Polypropylene (PP) fiber is one of the most widespread synthetic fibers. Owing to its good mechanical strength, low density, chemical resistance, thermal stability, and low cost, PP fiber is widely used in textile and filtration industries. Unfortunately, inherent hydrophobicity and radiation degradation of PP limit its use in hypaethral applications.¹

To improve the UV-resistance of fibers, a great deal of effort has been paid to relevant research. The titania (TiO_2) nanoparticles were one kind of commonly used UV-resistant additives and effective UV shielding agents to against the UV rays. Han *et al.*² dispersed the TiO_2 (treated with coupling agent) into ethylene glycol (EG) to react with terephthalic acid *via* polycondensation, and finally spun the PET/ TiO_2 nanocomposites into fibers. However, the TiO_2 nanoparticles in blending spinning solution will cause damage to the internal structure of the fiber,

Acknowledgments: This research is supported by the National Natural Science Foundation of China (Grant Nos. 21374078, 21174103 and 51303129), Science and Technology Commission Foundation of Tianjin (Grant Nos. 15JCYBJC17900 and 14JCZDJC38300) and the Program for Changjiang Scholars and Innovative Research Team in University (PCSIRT) of Ministry of Education of China (Grant No. IRT13084).

*Corresponding Authors: Xia Feng (fengxia@tjpu.edu.cn), Yiping Zhao (yipingzhao@tjpu.edu.cn)

resulting a significantly decrease in mechanical properties. Thus, this method was unsuitable for practical application. Instead, coating the fiber with functional materials was an effective method to overcome intrinsic deficiencies and introduce new properties to the final product. Previously, Tian *et al.*^{3,4} deposited graphene oxide and chitosan on the fabric substrate *via* layer-by-layer self-assembly and remarkably increased the UV-resistance of fabric. Nevertheless, the high cost and the complex steps limited its further application. Similarly, Xiao *et al.*⁵ coated a nanoscale TiO_2 coating on the silk fiber *via* atomic layer deposition. After modifying the TiO_2 -coated silk fiber possessed excellent UV protection properties, mechanical properties and minimal yellowing. Unfortunately, this method was not conducive to mass production for the long production cycle. Karimi *et al.*⁶ treated the cotton fabrics with TiO_2 nanosol, and then the fabrics were hot-pressed to improve self-cleaning and UV blocking properties. Although this method was widely implemented in research, the adhesion between TiO_2 and the substrate was generally unsatisfactory.

Recently, dopamine (DA), an amino acid in secreted mussel adhesive proteins, has attracted much attention for the strong adhesion to almost all types surface.⁷⁻¹⁰ In addition, the self-polymerization reaction of the dopamine was so mild (pH>7.5 with oxygen) without need for any complicated instrumentation or harsh reaction conditions.¹¹ Furthermore, many functional

groups (such as catechol, amine, and imine) on polydopamine (PDA) can serve as a versatile platform for secondary reactions and improve the wettability of the hydrophobic materials.¹²⁻¹⁵ It has been reported that PDA could react with the amine and/or thiol containing molecules through Michael addition or Schiff base reaction.¹⁶⁻²⁰ Especially, PDA could also resist the UV rays by quenching the reactive radicals, because its chemical structure was similar to that of eumelanins. Besides, the catechol on PDA has the ability to reduce metal ions or metal oxide and make it possible to deposit a metal oxide coating onto the substrates.^{21,22}

In this work, the UV-resistant PP fiber was fabricated through PDA functionalization followed by the deposition of TiO₂ nanoparticles. The PDA layer introduced plenty of amine and catechol groups onto the PP fiber, and these groups provided an important platform for secondary reactions of next step. Afterward, the TiO₂ nanoparticles were reduced in situ to the catechol groups in PDA, resulting in a TiO₂ layer on the fiber surface. The combination of PDA and TiO₂ nanoparticles endowed the PP fiber with excellent UV-resistant properties. In this approach, neither complex operation nor any extra energy was needed, and the process did not require the time-consuming synthesis and it was solvent free and non-toxic. Moreover, the TiO₂ was immobilized on fiber surface with chemical bonds, unlike the physical adhesion through blending modification. Herein, it was a promising and potential strategy to modify the PP fiber.

2. Experimental

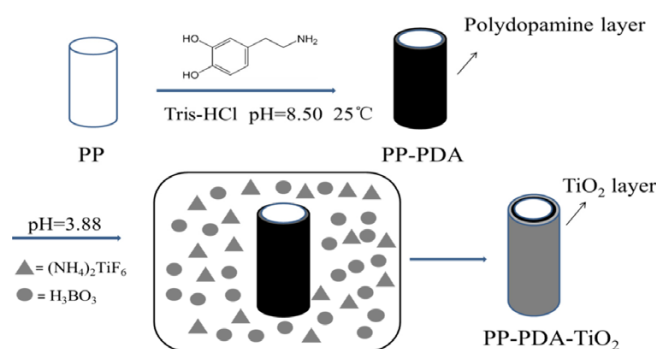
2.1. Materials

The PP fibers and nonwovens used in this study were supplied by Hainan Xinlong Nonwovens Co. Ltd. (Hainan China). Dopamine hydrochloride was purchased from Ouhe Technology Co. Ltd. (Beijing China). Tris (Ultra-Pure Grade) was purchased from Beijing Solarbio Technology Co. Ltd. (Beijing China). Boric acid was purchased from Letai Chemical Engineering Technology Co. Ltd. (Tianjin China). Ammonium hexafluorotitanate (Chemical Pure 98%) was purchased from Aladdin Reagent.

2.2. Preparation of UV-resistant PP fibers

Scheme 1 illustrated the detailed deposition process of PDA and TiO₂ coatings. Firstly, the PP fibers were cut into 15 cm and sonicated in ethanol for 30 min to remove the residual organic reagent. Then the fibers were rinsed with deionized water for several times, and dried in the blowing oven for 6 h at 60 °C.

The neat PP fibers were immersed in an aqueous solution of dopamine (2 mg/mL), buffered to a pH typical of marine environments (10 mM Tris, pH 8.50).¹³ The mixture was stirred at ambient temperature for 24 h. Subsequently, the fibers were washed thoroughly with deionized water and denoted as PP-PDA. When the PP fiber was dipped in dopamine solutions, covalent and noncovalent interactions between dopamine and the PP fiber were built up, making a PDA layer that was tightly stuck to the fiber surface.²³ In addition, the color of the dopa-



Scheme 1. Schematic illustration of preparation route of the PP-PDA-TiO₂.

mine solution displayed a visible alteration from colorless to pale brown and finally to deep brown. It inferred that the PDA was coated onto the fiber surface.²⁴

The resultant PP-PDA fibers were immersed in the (NH₄)₂TiF₆ (0.1 M) and H₃BO₃ (0.3 M) solution with a pH value of 3.88 at room temperature for 1 h, 3 h, 5 h, 7 h, 12 h. The TiO₂ nanoparticles were generated *via* the hydrolysis of (NH₄)₂TiF₆ and H₃BO₃, and then these nanoparticles were reduced in situ to the catechol groups in PDA. The immobilized TiO₂ nanoparticles performed as the seed layer to promote the homogeneous deposition of TiO₂. Eventually, a high-strength irreversible TiO₂ layer formed on PP fiber surface. These samples were rinsed, dried and denoted as PP-PDA-TiO₂.

2.3. Characterization

Surface morphologies of the pristine and modified fibers were observed and investigated *via* a scanning electron microscope (SEM, Hitachi S-4800, Japan) with an operating voltage of 10 kV.

Attenuated total reflectance fourier transform infrared spectroscopy (ATR-FTIR, NICOLET 6700, USA) was used to analyze the chemical structure of the fiber surface.

X-Ray photoelectron spectroscopy (XPS, Geneis 60S, USA) was used to investigate the chemical composition of the fiber surface with Al K α excitation radiation (1486.6 eV).

Thermogravimetry analysis was used to characterize the thermostability of the pristine and modified fibers. The parameter of this measurement was from room temperature to 800 °C with a heating rate of 10 °C/min in N₂.

X-Ray diffraction (XRD, D8 ADVANCE, USA) was used to characterize the crystalline structures of samples, and the diffraction patterns were recorded with the 2 θ range of 5-35°.

The pristine and the modified fibers were exposed to the UV light for 48 h. The distance to the UV light was fixed at 25 cm. The UV intensity on PP fiber was 80 W/m².

The mechanical properties were measured by a monofilament tensile machine (LLY-06, China) at a tensile speed of 5 mm/min and gauge length of 10 mm. The samples included the pristine and the modified fibers before and after UV exposure. The values of breaking strength and breaking elongation were obtained from the average of 15 measurements.

UV-Vis spectrophotometer (Lambda 35, PerkinElmer, Germany) was used to investigate the UV resistant property of sub-

strates. In order to characterize the UV-resistance of material conveniently, PP nonwoven fabrics were adopted and modified according to the method mentioned above.

3. Results and discussion

3.1. Chemical compositions of fiber surface

ATR-FTIR spectra of PP and PP-PDA were shown in Figure 1. It can be seen that the multiple peaks from 2800 cm^{-1} to 3000 cm^{-1} belonged to PP, including various mode stretching vibrational peaks of CH, CH₂, and CH₃. Moreover, the peaks at 1376 cm^{-1} and 1455 cm^{-1} were assigned to CH₃ and CH₂ bending vibration bands respectively. Except for the mutual peaks, the PP-PDA curve showed an additional peak at 1620 cm^{-1} , corresponding to the overlap of C=C resonance vibrations in aromatic ring and N-H bending vibrations, which were brought by PDA, indicating that the PDA was successfully coated onto the fiber surface. The chemical compositions of PP, PP-PDA, and PP-PDA-TiO₂ (1 h, 3 h, 5 h, 7 h, 12 h) samples were investigated by XPS analysis. The results of PP, PP-PDA, and PP-PDA-TiO₂-12h were shown in Figure 2. The detailed elements content of all samples were listed in Table 1. From Figure 2(a), C and O elements were found in the PP survey scan. The O elements in PP fiber were probably caused by additive added during production process or brought by the H₂O in the air. In the PP-PDA survey scan (Figure 2(c)), a visible N 1s peak was appeared and the relative amounts of O elements increased from 7.20% to 21.66% (Table 1), implying the PDA was coated on fiber surface. After

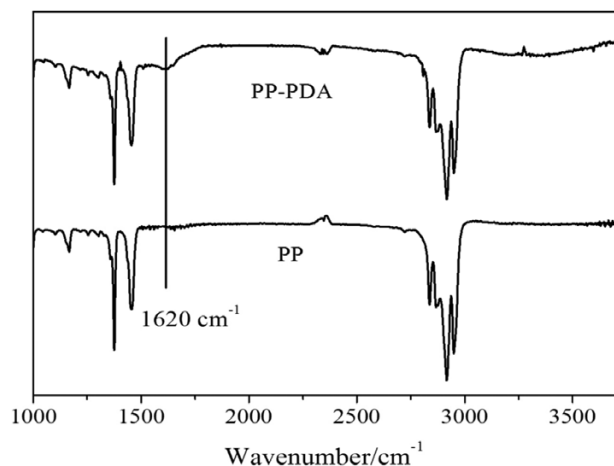


Figure 1. ATR-FTIR spectra of PP fiber and PP-PDA fibers.

Table 1. Elements composition of PP, PP-PDA, and PP-PDA-TiO₂ fibers with different reaction times

Sample	C (%)	O (%)	N (%)	Ti (%)
PP	92.80	7.20	-	-
PP-PDA	73.11	21.66	5.23	-
PP-PDA-TiO ₂ -1h	68.48	22.19	3.13	6.21
PP-PDA-TiO ₂ -3h	57.16	35.26	-	7.58
PP-PDA-TiO ₂ -5h	57.75	34.94	-	7.35
PP-PDA-TiO ₂ -7h	52.44	39.46	-	8.10
PP-PDA-TiO ₂ -12h	56.71	32.69	-	10.60

TiO₂ deposition, a remarkable Ti 2p peak emerged for the PP-PDA-TiO₂-12h fiber in Figure 2(e), and the relative content of O elements were further increased. As expected, the amount of Ti elements also raised with the increase of TiO₂ deposition time. High-resolution scans were performed around peaks of C 1s, N 1s, and Ti 2p respectively. As shown in Figure 2(b), the C 1s spectrum of PP had two peaks, one for the C-C at 285.1 eV and the other for the CH₂ at 286.6 eV. The C 1s spectrum of PP-PDA (Figure 2(d)) can be curve-fitted into four components with binding energies of approximately 285.1, 286.3, 287.3, 288.6 eV, corresponded to the C-C, C-N/C-O, C=O, O=C-N satellite species, which were formed during the dopamine oxidative polymerization. The C 1s spectrum of PP-PDA-TiO₂-12h (Figure 2(f)) contained only one peak component, which was attributed to the C-C species, at a binding energy of 285.0 eV. The N 1s spectrum of three samples was shown in Figure 2(g). The PP-PDA sample exhibited a peak at 400.1 eV due to the -NH- in PDA. Nevertheless, the N 1s peaks disappeared after the deposition of TiO₂, which was consistent with the fiber surface coated by the TiO₂ nanoparticles. From the Ti 2p spectrum (Figure 2(h)), it can be seen that two Ti 2p peaks emerged for the PP-PDA-TiO₂-12h fiber. The two peaks at 458.5 and 464.5 eV were assigned to Ti2p_{3/2} and Ti2p_{1/2} respectively, which were typical XPS spectra of Ti⁴⁺.⁸ As expected, the XPS analysis further verified the finding that both of the PDA and TiO₂ coatings were successfully deposited on PP fiber surface.

3.2. Crystalline structure and morphology of fiber surface

Crystalline structure of PP, PP-PDA, PP-PDA-TiO₂-5h were performed by XRD, the spectrum was shown in Figure 3. It can be found that there were three distinct characteristic peaks at 2θ values of 14° , 16.8° , 18.4° , respectively, corresponding to the (110), (040), and (130) planes of α -crystal forms of polypropylene. Furthermore, the three same curves with different intensity had no typical diffraction peaks for anatase or rutile TiO₂ on the PP-PDA-TiO₂-5h fiber. However, it was evidenced that the TiO₂ existed on fiber surface via XPS. Thus, with the combination of the XRD spectrum and the reaction temperature (room temperature) used in this paper, it can be concluded that the TiO₂ coatings was amorphous.

SEM images of pristine and modified fibers were shown in Figure 4. It can be seen in Figure 4(a) that the pristine PP fiber displayed a surface with some micropits and grooves. These micropits and grooves were probably the result of tensile crystallization in the processing of PP fiber.¹⁹ As shown in Figure 4(b), after dopamine oxidative polymerization, a uniform but rough PDA layer was formed on the PP fiber surface. The change in surface morphology further confirmed that PDA was successfully deposited on the fiber surface. The PDA layer provided a platform for secondary reaction, and the catechol groups in PDA reduced the TiO₂ nanoparticles in situ. The images of PP-PDA-TiO₂ fibers prepared at different time (1 h, 3 h, 5 h, 7 h, and 12 h) were shown in Figure 4(c)-(g). It can be seen from Figure 4(c) and (d) that the TiO₂ nanoparticles were small and individually distributed on the PP-PDA surface at a short reaction time of 1 h and 3 h. With the increase of reaction time from

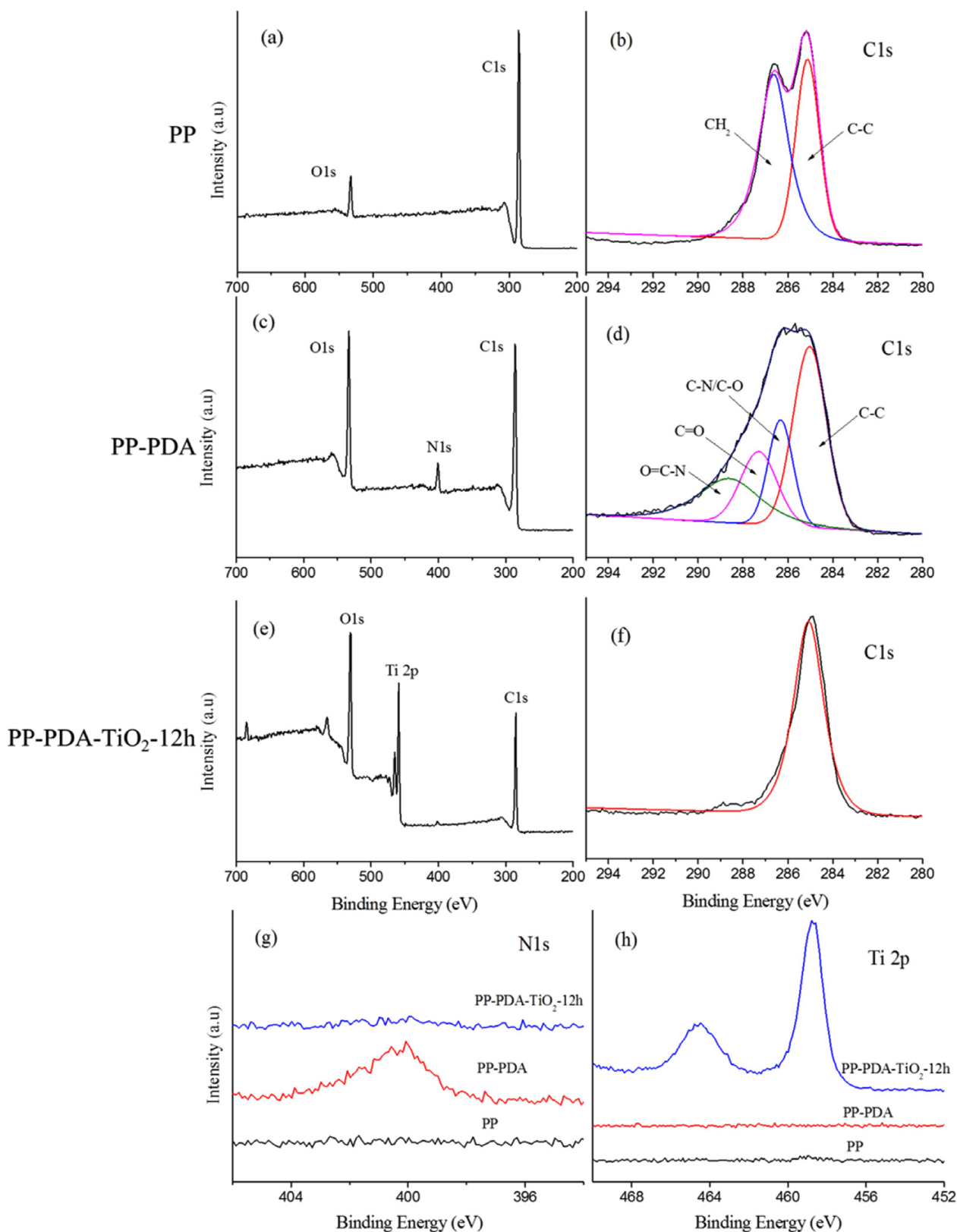


Figure 2. (a, c, e) XPS survey scan spectra, (b, d, f) C 1s spectra, (g) N 1s spectra, and (h) Ti 2p spectra of PP, PP-PDA, PP-PDA-TiO₂-12h fibers.

5 h to 12 h, the TiO₂ particle size and the thickness of TiO₂ coating increased gradually, resulting in the formation of a continuous and compact TiO₂ layer on fiber surface. With the extension of reaction time (as shown in Figure 4(f) and (g)), some significant cracks emerged in the TiO₂ coating. These cracks were mainly

caused by lateral shrinkage during the drying process. Additionally, the difference in coefficients of thermal expansion of TiO₂ coating and PP substrate may also one of the factors resulted the cracks.

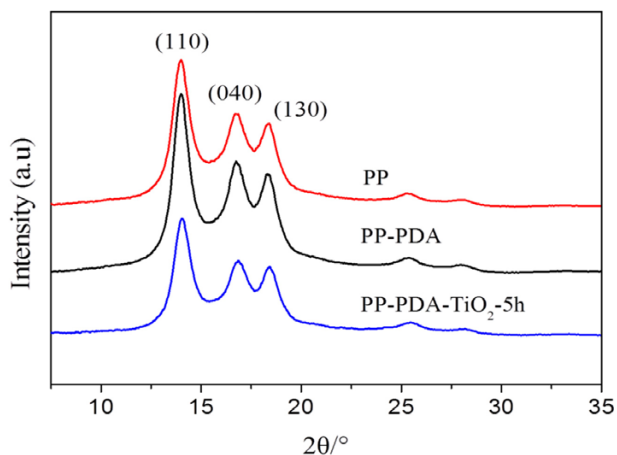


Figure 3. XRD spectra of PP, PP-PDA and PP-PDA-TiO₂-5h fibers.

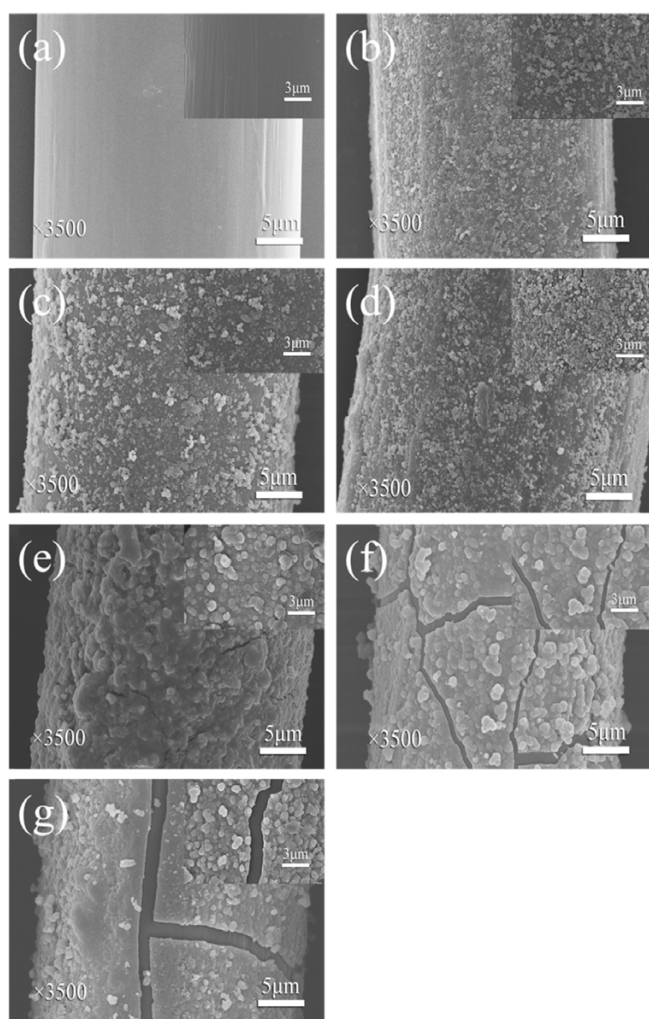


Figure 4. SEM images of (a) PP fiber, (b) PP-PDA fiber, and PP-PDA-TiO₂ fibers prepared at reaction time of (c) 1 h, (d) 3 h, (e) 5 h, (f) 7 h, and (g) 12 h.

3.3. Thermal stability of modified fiber

The thermo gravimetric analysis (TGA) and derivative thermo gravimetry (DTG) curves were shown in Figure 5(a),(b), respectively. From Figure 5(a), it can be found that the weight loss curves of the four samples exhibited similar two-stage process.

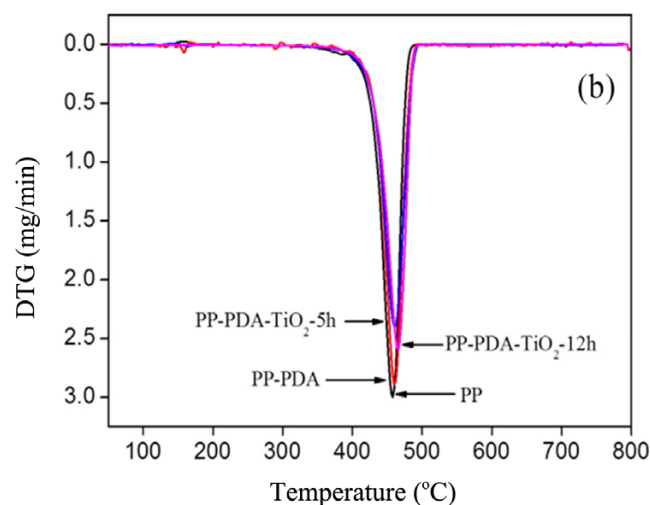
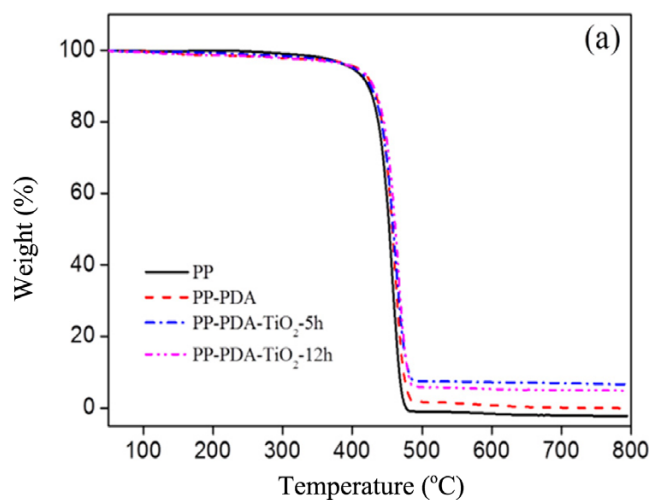


Figure 5. (a) Weight loss and (b) DTG spectra of PP, PP-PDA, PP-PDA-TiO₂-5h, and PP-PDA-TiO₂-12h fibers.

The weight loss between 30-350 °C was associated with the evaporation of the absorbed moisture on the fiber surface, and 350-500 °C was the major decomposition stage, which indicated the decomposition of the PP fiber. No further weight loss could be observed above 500 °C. The residual were TiO₂ particles. It can be found that the modified fibers had a higher decomposition temperature than that of the original fiber, and the decomposition temperature increased with the increase of TiO₂ deposition time. This was caused by the TiO₂ coating and the strong interactions (covalent bonds, noncovalent bonds and hydrogen bonds) between PDA and substrates. From the DTG curves, the PP-PDA-TiO₂-5h sample had a lower decomposition rate in comparison with the other samples, which was attributed to the TiO₂ layer performed as a protection layer to isolate the heat transfer and prevent fibers from being decomposed. The higher decomposition rate for PP-PDA-TiO₂-12h sample was mainly resulted by the cracks on TiO₂ coating. These cracks exposed fibers into the air and failed to protect it.

3.4. Mechanical property

The breaking strength and breaking elongation of original and modified fibers were shown in Figure 6(a) and (b). As shown in

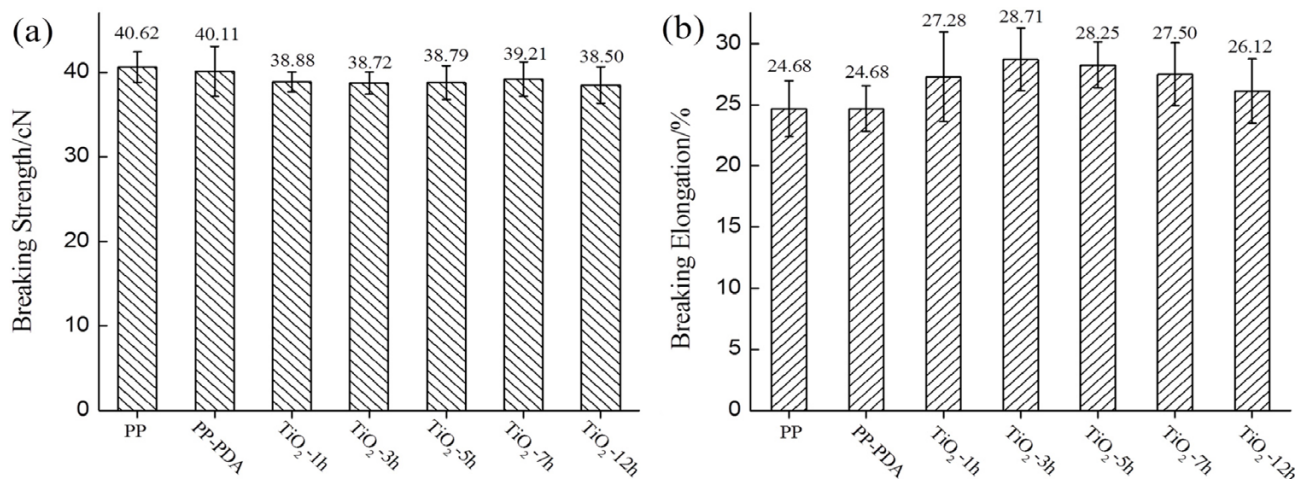


Figure 6. (a) Breaking strength and (b) breaking elongation of PP, PP-PDA, and PP-PDA-TiO₂ fibers prepared at 1 h, 3 h, 5 h, 7 h, and 12 h.

Figure 6(a), the breaking strength of modified fibers had no significant change in comparison with the pristine fiber. In fact, the PDA and TiO₂ coatings on the fiber surface would not affect the crystalline structure of the fibers. From Figure 6(b), the breaking elongation of fibers had an increase firstly from 24.7% to 28.7%, and then decreased to 26.1%, the maximum value was 28.7% (PP-PDA-TiO₂-3h). The increase was mainly caused by two aspects. On the one hand, some of inorganic small molecules, such as alkali or acid, infiltrated into inside of fibers and performed as the plasticizer to make the fibers more flexible; on the other hand, the PDA coating played a binder role in this system and provided a connecting force to prevent the fiber from being broken during the tensile process. For the samples of PP-PDA-TiO₂-7h and PP-PDA-TiO₂-12h, the breaking elongation decreased from 28.7% to 26.1%, since the TiO₂ coating grew over thick, and the fibers became hard and brittle. Generally, the mechanical properties of the fibers had no significant change before and after the modification, which confirmed that this modification method was a stable and mild approach to modify the PP fiber.

3.5. UV-Resistant properties

The mechanical properties of the pristine and the modified fibers before and after UV exposure were measured to explore the UV protection property of the TiO₂ coating. The results were shown in Figure 7(a),(b) and the detailed data was listed in Table 2 and Table 3. From Figure 7(a), it can be seen that after UV exposure 48 h, the breaking strength of the pristine PP fiber decreased sharply from 40.62 cN to 32.12 cN (the decrease value was 8.50 cN). The PP-PDA fiber had a lower decrease in breaking strength (the value was 7.60 cN) in comparison with the PP fiber. However, the TiO₂-coated fibers maintained relatively high breaking strength. Furthermore, from PP-PDA-TiO₂-1h to PP-PDA-TiO₂-12h, the breaking strength increased gradually. In particular, the PP-PDA-TiO₂-12h sample scarcely changed (the decrease value was only 1.01 cN) in breaking strength after the UV treatment, indicating that the TiO₂ coating could effectively resist the UV irradiation. As to Figure 7(b), it can be seen that the breaking elongation after UV exposure presented

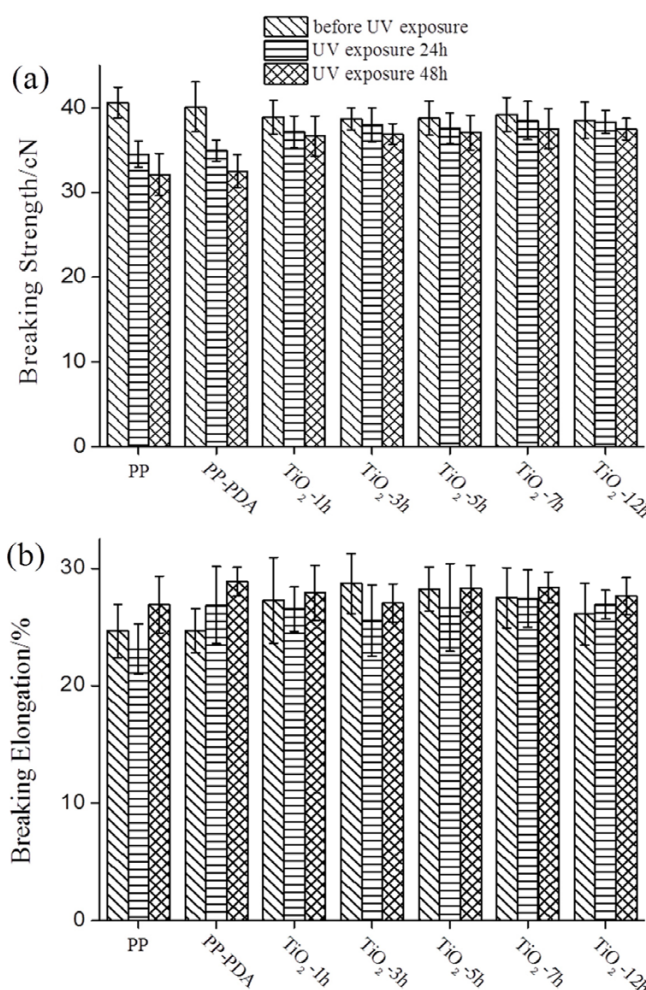


Figure 7. (a) Breaking strength and (b) breaking elongation of PP, PP-PDA, and PP-PDA-TiO₂ fibers before and after UV exposure.

a similar trend to the breaking strength. Therefore, it can be concluded that the TiO₂ coating could absorb and reflect the UV rays, and provided an excellent UV protection property to the fiber.

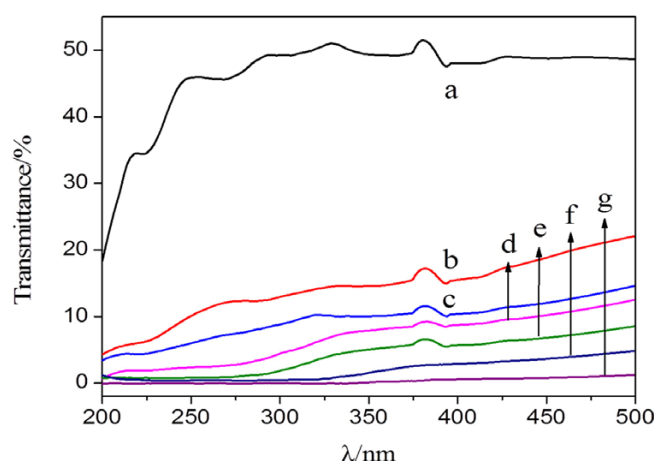
The UV transmittance was measured by using PP nonwoven fabric, the result was shown in Figure 8. Obviously, the PP-PDA

Table 2. The breaking strength of PP, PP-PDA, and PP-PDA-TiO₂ fibers before and after UV exposure

Sample	Breaking strength (cN)		
	Before UV Exposure	UV Exposure 24 h	UV Exposure 48 h
PP	40.62 ± 1.82	34.52 ± 1.56	32.12 ± 2.48
PP-PDA	40.11 ± 2.95	34.94 ± 1.24	32.52 ± 1.96
PP-PDA-TiO ₂ -1h	38.88 ± 2.00	37.15 ± 1.51	36.66 ± 2.36
PP-PDA-TiO ₂ -3h	38.72 ± 1.31	37.99 ± 1.99	36.68 ± 1.25
PP-PDA-TiO ₂ -5h	38.79 ± 2.01	37.57 ± 1.83	37.08 ± 2.06
PP-PDA-TiO ₂ -7h	39.21 ± 2.04	38.52 ± 2.26	37.51 ± 2.38
PP-PDA-TiO ₂ -12h	38.50 ± 2.15	38.34 ± 1.36	37.49 ± 1.27

Table 3. The breaking elongation of PP, PP-PDA, and PP-PDA-TiO₂ fibers before and after UV exposure

Sample	Breaking elongation (%)		
	Before UV Exposure	UV Exposure 24 h	UV Exposure 48 h
PP	24.68 ± 2.28	23.11 ± 2.15	26.91 ± 2.41
PP-PDA	24.68 ± 1.87	26.87 ± 3.29	28.86 ± 1.24
PP-PDA-TiO ₂ -1h	27.28 ± 3.66	26.54 ± 1.88	27.91 ± 2.37
PP-PDA-TiO ₂ -3h	28.71 ± 2.55	25.57 ± 3.04	27.06 ± 1.64
PP-PDA-TiO ₂ -5h	28.25 ± 1.88	26.68 ± 3.76	28.28 ± 1.99
PP-PDA-TiO ₂ -7h	27.50 ± 2.56	27.45 ± 2.48	28.37 ± 1.32
PP-PDA-TiO ₂ -12h	26.12 ± 2.63	26.91 ± 1.22	27.65 ± 1.57

**Figure 8.** UV-Vis transmittance spectra of (a) PP, (b) PP-PDA and PP-PDA-TiO₂ nonwoven fabrics prepared at (c) 1 h, (d) 3 h, (e) 5 h, (f) 7 h, and (g) 12 h.

nonwoven fabric had a remarkable decrease in transmittance, comparing to the PP sample. It suggested that the PDA also had the capacity to resist the UV rays. It has been reported that the PDA could quench the reactive radicals generated by UV radiation,²⁵⁻²⁷ and the PDA layer was served as free-radical scavenger on the fiber surface. The UV transmittance of the PP-PDA-TiO₂-1 h nonwoven fabric was further decreased in comparison with the PP-PDA. As known to us, the TiO₂ nanoparticles were an effective UV shielding agent to reflect and absorb the UV rays. The TiO₂ coating could transform the UV rays into heat and visible light, and reduced the transmitted light to minimum. In addition, the transmittance decreased gradually from PP-PDA-TiO₂-1h to PP-PDA-TiO₂-12h, and finally reduced to 0% for the PP-PDA-TiO₂-12h nonwoven fabric, implying that the modified samples obtained excellent UV-resistance proper-

ties. It also can be seen that the transmittance was in a low degree in the visible region (>400 nm), indicating that the TiO₂ coating could reflect or scatter the visible light. By the way, the small peaks around 270-390 nm maybe the result of additives and organic residue in fibers, which was consistent with the XPS analysis of PP fiber. Consequently, it can be concluded that both of the PDA and the TiO₂ layers showed good UV-resistant capacity. The synergistic effect of the two layers vested the fabric with excellent UV-resistant properties.

4. Conclusions

In conclusion, this study carried out a mild and environment-friendly strategy to fabricate the UV-resistance fibers. The PDA and TiO₂ were coated on fiber surface simply *via* immersing the fiber into relevant solutions. Thermal stability was investigated and the result suggested that the decomposition temperature and decomposition rate were improved after modification. The excellent UV-Vis protection property of the modified fiber was manifested in UV transmittance. Especially, the UV transmittance of the PP-PDA-TiO₂-12h nonwoven fabric was reduced to 0% with no obvious change in mechanical properties. This method can be extended and used in other fibers for various applications.

References

- (1) K. K. Goli, O. J. Rojas, and J. Genzer, *Biomacromolecules*, **13**, 3769 (2012).
- (2) K. Han and M. Yu, *J. Appl. Polym. Sci.*, **100**, 1588 (2006).
- (3) M. Tian, X. Hu, L. Qu, L. Qu, S. Zhu, Y. Sun, and G. Han, *Carbon*, **96**, 1166 (2016).
- (4) M. Tian, X. Hu, L. Qu, L. Qu, S. Zhu, Y. Sun, and G. Han, *Appl. Surf. Sci.*, **377**, 141 (2016).

- (5) X. Xiao, X. Liu, F. Chen, D. Fang, C. Zhang, L. Xia, and W. Xu, *ACS Appl. Mater. Interfaces*, **7**, 21326 (2015).
- (6) L. Karimi, S. Zohoori, and A. Amini, *New Carbon Mater.*, **29**, 380 (2014).
- (7) H. Lee, N. F. Scherer, and P. B. Messersmith, *Proc. Natl. Acad. Sci. U.S.A.*, **103**, 12999 (2006).
- (8) Q. Ye, F. Zhou, and W. Liu, *Chem. Soc. Rev.*, **40**, 4244 (2011).
- (9) B. Bhushan, *Langmuir*, **28**, 1698 (2012).
- (10) E. Faure, C. Falentin-Daudré, C. Jérôme, J. Lyskawa, D. Fournier, P. Woisel, and C. Detrembleur, *Prog. Polym. Sci.*, **38**, 236 (2013).
- (11) J. Sedó, J. Saiz-Poseu, F. Busqué, and D. Ruiz-Molina, *Adv. Mater.*, **25**, 653 (2013).
- (12) D. R. Dreyer, D. J. Miller, B. D. Freeman, D. R. Paul, and C. W. Bielawski, *Langmuir*, **28**, 6428 (2012).
- (13) H. Lee, S. M. Dellatore, W. M. Miller, and P. B. Messersmith, *Science*, **318**, 426 (2007).
- (14) J. H. Waite, *Nat. Mater.*, **7**, 8 (2008).
- (15) M. Xie, J. Wang, X. Wang, M. Yin, C. Wang, D. Chao, and X. Liu, *Macromol. Res.*, **24**, 965 (2016).
- (16) Y. Liu, K. Ai, and L. Lu, *Chem. Rev.*, **114**, 5057 (2014).
- (17) M. Hu and B. Mi, *Environ. Sci. Technol.*, **47**, 3715 (2013).
- (18) L. Wang, D. Wang, Z. Dong, F. Zhang, and J. Jin, *Nano Lett.*, **13**, 1711 (2013).
- (19) L. Xu, W. Yang, K. G. Neoh, E. Kang, and G. Fu, *Macromolecules*, **43**, 8336 (2010).
- (20) J. H. Jegal, G. H. Choi, H. J. Lee, K. D. Kim, and S. C. Lee, *Macromol. Res.*, **24**, 83 (2016).
- (21) W. Wang, R. Li, M. Tian, L. Liu, H. Zou, X. Zhao, and L. Zhang, *ACS Appl. Mater. Inter.*, **5**, 2062 (2013).
- (22) S. H. Yang, S. M. Kang, K. Lee, T. D. Chung, H. Lee, and I. S. Choi, *J. Am. Chem. Soc.*, **133**, 2795 (2011).
- (23) X. Xu, B. Bai, C. Ding, H. Wang, and Y. Suo, *Ind. Eng. Chem. Res.*, **54**, 3268 (2015).
- (24) Y. Liao, Y. Wang, X. Feng, W. Wang, F. Xua, and L. Zhang, *Mater. Chem. Phys.*, **121**, 534 (2010).
- (25) P. Meredith and T. Sarna, *Pigm. Cell Melanoma R.*, **19**, 572 (2006).
- (26) K. Shanmuganathan, J. H. Cho, P. Iyer, S. Baranowitz, and C. J. Ellison, *Macromolecules*, **44**, 9499 (2011).
- (27) K. Ju, Y. Lee, S. Lee, S. B. Park, and J. Lee, *Biomacromolecules*, **12**, 625 (2011).